Edge Electrostatic Fluctuations and Transport in a Reversed-Field Pinch

T. D. Rempel, C. W. Spragins, S. C. Prager, S. Assadi, D. J. Den Hartog, and S. Hokin
University of Wisconsin–Madison, Madison, Wisconsin 53706
(Received 15 April 1991)

Electrostatic fluctuations have been measured in a large reversed-field pinch, and are large ($\tilde{n}_e/n \sim 20\%$–40%, $\tilde{T}_e/T \sim 10\%$–25%). Frequency and wave-number spectra are broad ($\Delta n \sim 70$–150, $\Delta m \sim 3$–6), and differ from measured magnetic fluctuation spectra. The transport inferred from correlation measurements indicates that electrostatic fluctuations can account for significant particle losses, but contribute $< 15\%$ to energy loss.

PACS numbers: 52.55.–s

In toroidal magnetic confinement devices, cross-field transport exceeds diffusion predicted by collisional processes. Some theoretical models invoke electrostatic turbulence to explain this anomalous transport. Charge separation results in a fluctuating electric field, $\tilde{\mathbf{E}} = -\nabla\tilde{\Phi}$; the $\tilde{\mathbf{E}}\times\mathbf{B}$ drift then drives transport. Electrostatic fluctuations may be responsible for particle transport in tokamak [1–4] and stellarator [5] edge plasmas, and perhaps also energy transport. Early measurements on ZETA [6] indicated that the role of electrostatic losses could be significant. More recent investigations have begun in several reversed-field-pinch (RFP) experiments [7–9]. The RFP and tokamak have similar edge plasma equilibrium density and temperature. However, the RFP contains greater magnetic shear, unfavorable magnetic curvature, and fewer magnetically trapped particles.

In this Letter, we report measurements of edge electrostatic fluctuations (in density, potential, and electron temperature) in the MST RFP. We find that the amplitudes are large and the frequency and wave-number spectra are broad, similar to fluctuations in tokamaks. The deduced fluctuation-induced particle transport is comparable to the total particle losses. However, the fluctuation-induced energy transport is relatively small.

MST [10,11] is a large RFP ($a = 0.52$ m, $R = 1.5$ m), with typical plasma parameters $I_p \leq 600$ kA, $\bar{n}_e = (0.5$–$2.0)\times 10^{13}$ cm^{-3}, $T_{e0} \leq 500$ eV, and pulse length ≤ 80 msec. The present studies were conducted in low-current plasmas [$I_p \leq 250$ kA, $\bar{n}_e = (0.6$–$0.8)\times 10^{13}$ cm^{-3}, $T_{e0} \leq 180$ eV], shown in Fig. 1. For these conditions, a single-turn loop voltage $V_l = 15.5$ V, pinch parameter $\Theta = B_p(a)/\langle B_t\rangle = 1.85$ (where $\langle B_t\rangle$ is the volume-averaged toroidal field), and reversal parameter $F = B_t(a)/\langle B_t\rangle = -0.15$ were obtained.

Probe measurements were made at $r/a \geq 0.92$ (where $r/a \equiv 1$ at the wall), 40° above the outer midplane. Graphite toroidal rail limiters extend 1 cm from the wall at the inner and outer midplane. Triple probes were constructed using 0.5-mm-diam tungsten tips, spaced 1.6 mm apart. Two triple clusters, separated by 11.4 mm, were fixed on a single probe support. Measurements were made using a triple probe technique [12]. Ion saturation current J_s was collected by a floating double probe biased to -300 V [$\geq (5$–$10)kT_e$]. The floating potential V_f was measured across a 100 kΩ impedance to the ground. The local plasma density n_e, electron temperature T_e, and plasma potential Φ_{pl} were then inferred by

$$k_B T_e = \beta e(V_e - V_f), \quad n = \zeta J_s (M_i/T_e)^{1/2}, \qquad e\Phi_{pl} = eV_f + \alpha k_B T_e, \tag{1}$$

where k_B is Boltzmann's constant, V_e is the potential of the positive-biased tip, and α, β, and ζ are constants. Allowing for effects due to probe geometry, sheath expansion [13], and secondary electron emission from thermal electrons, the values $\alpha \sim 2$, $\beta \sim 1$, and $\zeta \sim 1$ were used [14]. Use of the ideal values of $\alpha = 3.3$, $\beta = 1/\ln 2$, and $\zeta = \sqrt{2}$ yielded a 20% difference in the calculated radial particle losses.

Exact determination of these coefficients is complicated by thermionic and secondary electron emission caused by nonthermal edge electrons, which are known to exist in MST [15] and other RFP's. We have made simple estimates of these effects using a hot-electron secondary-emission coefficient of ~ 1.3 and allowing for possible space-charge limitations on this emission. For average hot-electron temperatures of 10–20 times the thermal electron temperature in the edge and densities 2%–3% of the background plasma density, the resulting error is $\leq 25\%$ in α, $\leq 10\%$ in β, and $< 20\%$ in ζ.

Data were digitized at a frequency of 1 MHz. Three-pole filtering with a 3-dB corner at 300 kHz was used. For statistical analysis of the fluctuations, several hundred time series data records were typically used, with several records taken from each shot. Analysis was restricted to time intervals in which the plasma current was within 10% of its peak value. Modes were assumed to be

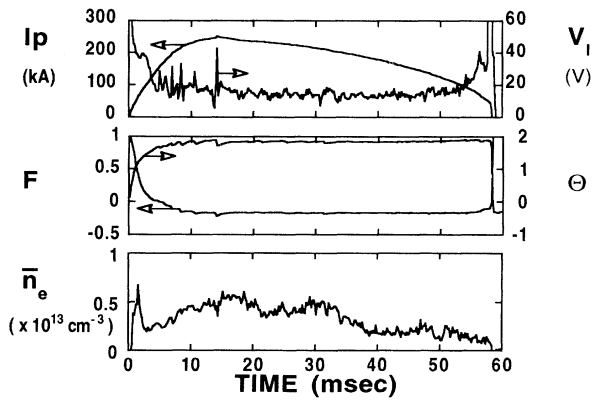

FIG. 1. Wave forms of I_p and V_l, F and Θ, and $\bar{n}_e$.

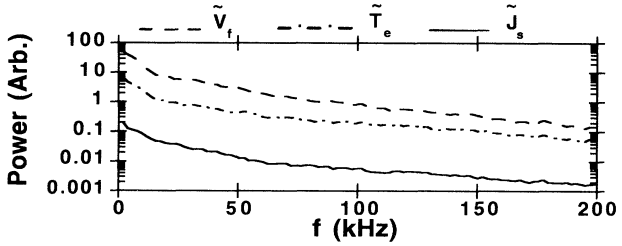

FIG. 2. Fluctuation power spectra of $\tilde{V}_f$ (---), $\tilde{T}_e$ (-·-·), and $\tilde{J}_s$ (——).

stationary over the 512 msec width of each record.

Electrostatic fluctuations in the edge of MST are broadband and turbulent. Typical power spectra, shown in Fig. 2, peak at low frequencies and fall monotonically with frequency. Radial profiles of relative fluctuation amplitudes (2–200 kHz) are shown in Fig. 3. The fluctuation amplitudes shown in Fig. 3(a) are large, with $|\tilde{n}_e|/n \sim 20\%$–$40\%$ and $|\tilde{T}_e|/T \sim 10\%$–$25\%$. The relative fluctuation levels increase with radius except at $r/a = 0.92$. Pressure fluctuation amplitudes also vary widely, $|\tilde{P}_e|/P \sim 20\%$–$50\%$. Plasma potential fluctuation amplitudes, $e|\tilde{\Phi}_{\rm pl}|/k_B T$, tend to be rather uniform outside $r/a = 0.92$. Within uncertainties, we find no significant evidence that force balance, $|\tilde{P}_e|/P \sim e|\tilde{\Phi}_{\rm pl}|/k_B T$, is violated [Fig. 3(b)].

To compare to measurements of magnetic fluctuation spectra on MST [16,17], the wave-number-frequency spectra have been approximated using two-point phase-shift measurements [18]. The resulting toroidal mode number spectra are shown in Fig. 4 (with $n = k_\phi R$, where ϕ indicates the toroidal direction). At low frequencies (10–25 kHz), electrostatic n spectra are broad, with a width $\Delta n \sim 70$ [Figs. 4(a) and 4(b)]. This is in contrast to the radial magnetic-field fluctuation n spectrum, which is dominated by a tearing mode peak at $n \sim 2R/a \sim 6$ and $\Delta n \leq 10$.

At higher frequencies (50–100 kHz), the electrostatic n spectra broaden even further to $\Delta n \sim 150$. At these frequencies, the n spectrum for $\tilde{V}_f$ tends to peak in the ion drift direction at $n \sim 10$–30 ($k_\phi \rho_s \sim 0.05$–0.15, where $\rho_s \sim 0.8$ cm in the edge). Because of uncertainties in the phase-shift measurement, this value is at the limits of the diagnostic accuracy. The n spectrum for $\tilde{J}_s$ shifts to the electron drift direction, peaking at $n \sim 10$–40. While the $\tilde{B}_r$ spectrum also shows a similar shift in this frequency band, the width is significantly smaller, $\Delta n \sim 60$.

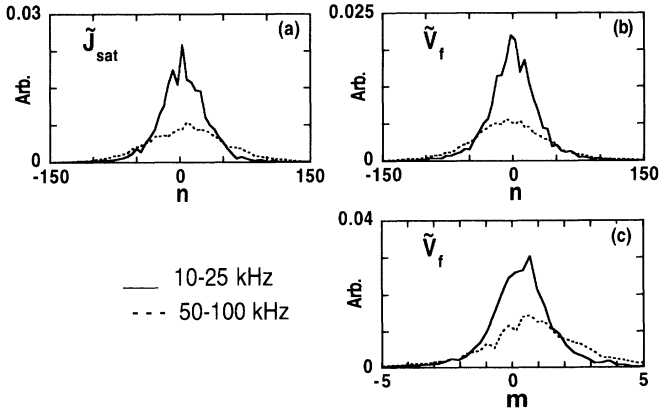

FIG. 4. Low- and high-frequency n spectra for (a) $\tilde{J}_s$ and (b) $\tilde{V}_f$, and (c) m spectra for $\tilde{V}_f$.

Poloidal mode spectra for $\tilde{V}_f$ [Fig. 4(c)], obtained from measurements using two electrostatic probes separated by 19 cm, show a much narrower width. At low frequencies, the spectrum is centered at $m = 1$ and has $\Delta m \sim 3$. The spectrum again broadens with frequency, to a width of $\Delta m \sim 6$, peaked at $m = 1$–2, at 50–100 kHz. While showing some general similarities to the electrostatic m spectra, the m spectra for $\tilde{B}_r$ are much more sharply peaked about $m = 1$, especially at low frequencies where $\Delta m \sim 1$.

The contrast between electrostatic and magnetic mode spectra might imply that the two are uncorrelated. Indeed, we measure that $\tilde{J}_s$ and $\tilde{B}_r$ are weakly correlated, as illustrated in Fig. 5. Although there is strong coherence between each of two closely spaced electrostatic and magnetic signals, the cross coherence between $\tilde{J}_s$ and $\tilde{B}_r$ is only modest, and only at low frequency, where the magnetic fluctuations are large.

The radial particle and energy flux generated by an $\tilde{\mathbf{E}} \times \mathbf{B}$ drift were calculated from $\Gamma_p = \langle \tilde{n}_e \tilde{v}_r \rangle$ and $Q_E = 3\langle \tilde{P}_e \tilde{v}_r \rangle/2$. Using $\tilde{\mathbf{v}}_r = \tilde{\mathbf{E}} \times \mathbf{B}/B^2$ and $\tilde{\mathbf{E}} = -i\mathbf{k}_\phi \tilde{\Phi}_{\rm pl}$, the spectral representations are [19]

$$\Gamma_p = \mathrm{Im}\langle \tilde{n}_e(f)^* k_\phi(f) \tilde{\Phi}_{\rm pl}(f) \rangle / B \,, \tag{2}$$

$$Q_E = 3\,\mathrm{Im}\langle \tilde{P}_e(f)^* k_\phi(f) \tilde{\Phi}_{\rm pl}(f) \rangle / 2B \,, \tag{3}$$

where nonsubscripted symbols represent mean quantities, and $\langle\,\rangle$ denotes an ensemble average. We have neglected

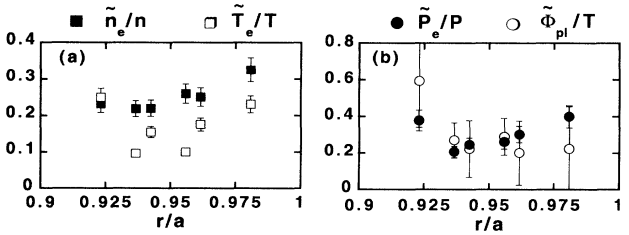

FIG. 3. Relative fluctuation amplitudes of (a) $\tilde{n}_e/n$ (■), $\tilde{T}_e/T$ (□) and (b) $\tilde{P}_e/P$ (●), $e\tilde{\Phi}_{\rm pl}/k_B T$ (○).

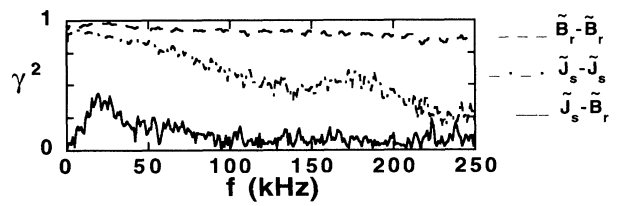

FIG. 5. Squared coherence (γ^2) of two $\tilde{B}_r$ (---) and of two $\tilde{J}_s$ (-·-·), each separated toroidally by 1.8 cm, and between $\tilde{B}_r$ and $\tilde{J}_s$ separated by 0.5 cm (——).

the component due to poloidal fluctuating electric field, which was found to be smaller by a factor of 100. Using Eqs. (1), the radial fluxes were then found from the measured $\tilde{J}_s$, $\tilde{V}_f$, and $\tilde{T}_e$ by

$$\Gamma_p = n \operatorname{Im}\left[\frac{\langle \tilde{J}_s^* k_V \tilde{V}_f\rangle}{JB} - \frac{\langle \tilde{T}_e^* k_V \tilde{V}_f\rangle}{2TB} + \alpha \frac{\langle \tilde{J}_s^* k_T k_B \tilde{T}_e\rangle}{eJB}\right], \tag{4}$$

$$Q_E = \frac{3P}{2} \operatorname{Im}\left[\frac{\langle \tilde{J}_s^* k_V \tilde{V}_f\rangle}{JB} + \frac{\langle \tilde{T}_e^* k_V \tilde{V}_f\rangle}{2TB} + \alpha \frac{\langle \tilde{J}_s^* k_T k_B \tilde{T}_e\rangle}{eJB}\right], \tag{5}$$

where the wave numbers k_V and k_T characterize $\tilde{V}_f$ and $\tilde{T}_e$, respectively. However, since measurements of spatial differences in $\tilde{T}_e$ are dominated by significant uncertainties, we have assumed $k_T = k_V$.

The squared coherence between $\tilde{J}_s$ and $-\nabla\tilde{\Phi}_f$ is modest; $\gamma^2 = \langle \tilde{J}_s^* k_V \tilde{V}_f\rangle / |\tilde{J}_s||\tilde{V}_f| \leq 0.1$–$0.4$, and decreases with radius. The cross power terms involving temperature fluctuations in Eqs. (4) and (5) can be important. The third term in these equations can contribute an inward flux of both particles and energy, and is nearly 100% of the first term at larger radii. At $r/a = 0.92$, however, this third term adds only a 10% effect. The second term in Eq. (4) contributes an additional outward flux of particles of 30%–50% of the first term. Figure 6(a) illustrates the contributions of $\tilde{T}_e$ to the total particle flux at $r/a = 0.94$.

The total calculated radial particle flux Γ_p, shown in Fig. 7(a), is observed to decrease with radius at the edge, as seen in tokamaks as well [2]. From the calculated flux at $r/a = 0.92$, a global particle confinement time limited to electrostatic losses was estimated as $\tau_p = N/4\pi^2 rR\Gamma_p \lesssim 1$ msec, where N was determined from $\bar{n}_e$ assuming a parabolic profile, and toroidal and poloidal symmetry was assumed. This confinement time is comparable to estimates of τ_p obtained from a 1D particle/neutral transport code with source terms inferred from inverted H_α emission profiles.

The decrease in fluctuation-induced flux with radius indicates that an additional plasma loss channel, which is believed to be scrape-off effects of the toroidal rail limiter, dominates near the tank wall. A simple model of 1D particle balance in an edge scrape-off layer, $\nabla\cdot\Gamma_p = S_i$, with parallel convection at the ion sound speed and radial transport due solely to electrostatic fluctuations, yields

$$\frac{\Gamma_p}{\lambda_\Gamma} + \frac{\zeta n_e [T_L/M_i]^{1/2}}{L} = S_i, \tag{6}$$

where $2L$ is the total scrape-off length in the edge, T_L is the electron temperature at the limiter, and λ_Γ is the radial scale length of the calculated flux. Using the measured $\lambda_\Gamma = 0.8$ cm and S_i, as determined from H_α emission, and assuming $T_L = 20$ eV, Eq. (6) then yields $L \sim 150$ cm, which is comparable to the distance along field lines between limiters.

The separate contributions of $\langle \tilde{n}_e \tilde{v}_r\rangle$ and $\langle \tilde{T}_e \tilde{v}_r\rangle$ to the total energy flux spectrum are shown in Fig. 6(b), and the total energy flux is shown in Fig. 7(b). A global energy confinement time from fluctuations has been calculated using the estimate $\tau_{Ee} = \frac{3}{2} NT_{e0}/4\pi^2 rRQ_E$, where a parabolic profile in temperature has also been assumed. When simple convection based on the first term in Eq. (5) was assumed, and $\tilde{T}_e$ effects were ignored, energy confinement times of ~ 4 msec or larger were calculated. However, temperature fluctuations add an inward energy flux, resulting in $\tau_{Ee} \sim 7$ msec at $r/a = 0.92$. This is significantly larger than the global energy confinement time in MST of ~ 0.5–1 msec at low plasma currents.

In summary, we find that fluctuation amplitudes of electron density and temperature in the edge of MST are large, with $|\tilde{n}_e|/n \sim 20\%$–$40\%$, and $|\tilde{T}_e|/T \sim 10\%$–$25\%$. No significant evidence for violation of force balance along the magnetic field is found. Toroidal and poloidal mode spectra for electrostatic signals have been measured. The spectra are broad and centered nearly at $m = 1$, $n = 0$, although some shift at higher frequency exists. This is in contrast to observed radial magnetic-field fluctuation spectra. Indeed, correlations between electrostatic ($\tilde{J}_s$) and magnetic ($\tilde{B}_r$) fluctuations are small in the edge of MST. Measured fluctuation-induced radial particle losses limit the particle confinement time to ~ 1 msec, which is comparable to the total particle confine-

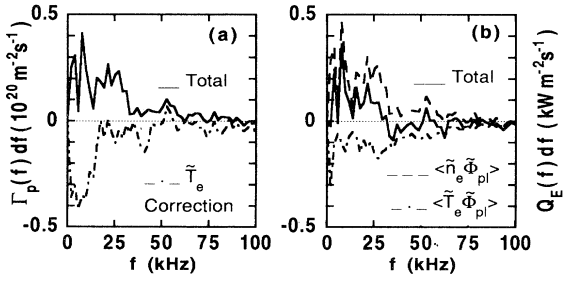

FIG. 6. Frequency spectra of (a) Γ_p (——) and $\tilde{T}_e$ effects (-·-·), and of (b) Q_E (——), and $\tilde{n}_e$ (---) and $\tilde{T}_e$ (-·-·) contributions to Q_E.

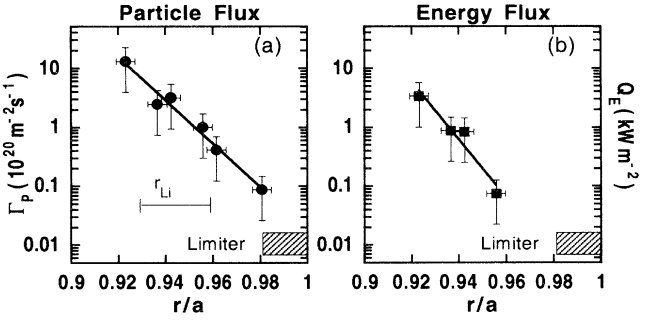

FIG. 7. Radial profiles of (a) Γ_p (●) and (b) Q_E (■).

ment time. Electrostatic energy fluxes are relatively small, contributing less than 15% of the global energy transport.

If one were to attribute transport in the RFP only to electrostatic and magnetic fluctuations, then our results would imply that magnetic fluctuations do not contribute substantially to particle transport. This is sometimes anticipated to be the case in view of ambipolarity constraints for either localized modes or global tearing modes. However, the relatively large magnetic fluctuations might still drive significant energy transport.

Despite the geometric difference between the RFP, tokamak, and stellarator, there is a qualitative similarity in the amplitude and spectral breadth of edge electrostatic fluctuations in the three configurations. Moreover, it appears that the edge energy transport in the RFP from electrostatic fluctuations alone might be of similar magnitude to the transport in a tokamak or stellarator of similar minor radius and plasma current (but higher magnetic field).

We are grateful for contributions of Dr. J. Sarff, Dr. A. Almagri, M. Stoneking, and the members of the MST group, and to Professor P. Terry. We thank Dr. S. Martini and Dr. P. Innocente of the Istituto Gas Ionizatti, Padova, Italy for interferometric density measurements in MST. This work was supported by the U.S. Department of Energy.

[1] S. J. Zweben *et al.*, J. Nucl. Mater. **111-112**, 39 (1982).
[2] W. L. Rowan *et al.*, Nucl. Fusion **27**, 1105 (1987).
[3] S. J. Levinson *et al.*, Nucl. Fusion **24**, 527 (1984).
[4] A. A. Howling and D. C. Robinson, in *Proceedings of the Workshop on Tubulence and Anomalous Transport in Magnetized Plasmas, Cargese, France, 1986,* edited by D. Gresillon and M. Dubois (Editions de Physique, Paris, 1986), p. 115.
[5] T. Uckan *et al.*, J. Nucl. Mater. **176-177**, 693 (1990).
[6] D. C. Robinson and M. G. Rusbridge, Plasma Phys. **11**, 73 (1969).
[7] C. W. Spragins *et al.*, Bull. Am. Phys. Soc. **34**, 2107 (1989).
[8] H. Toyama and H. Ji, in Proceedings of the Transport Task Force Workshop, South Carolina, 1990 (unpublished).
[9] H. Y. W. Tsui *et al.*, Bull. Am. Phys. Soc. **35**, 2027 (1990).
[10] R. N. Dexter *et al.*, Fusion Tech. **19**, 131 (1991).
[11] S. C. Prager *et al.*, Phys. Fluids B **2**, 1367 (1990).
[12] S. L. Chen and T. J. Sekiguchi, J. Appl. Phys. **36**, 2363 (1965).
[13] J. G. Laframboise, University of Toronto Report No. UTIAS 100, 1966 (unpublished).
[14] T. D. Rempel, University of Wisconsin–Madison, Department of Physics, Plasma Report No. PLP 1083, 1991 (unpublished).
[15] A. Almagri *et al.*, "Global Confinement in the MST Reversed Field Pinch," in Proceedings of the Workshop on Physics of Alternative Confinement Schemes, Varenna, 1990 (to be published).
[16] A. Almagri *et al.*, "Edge Fluctuations in the MST Reversed Field Pinch," in Proceedings of the Workshop on Physics of Alternative Confinement Schemes, Varenna, 1990 (to be published).
[17] S. C. Prager, Plasma Phys. Controlled Fusion **32**, 903 (1990).
[18] J. M. Beall *et al.*, J. Appl. Phys. **53**, 3933 (1982).
[19] Ch. P. Ritz *et al.*, Rev. Sci. Instrum. **59**, 1735 (1988).